Int. J. Electrochem. Sci., 6 **(2011)** 889 - 900

International Journal of
ELECTROCHEMICAL
SCIENCE
www.electrochemsci.org

A Reactive Methanol Filter with a Layer of Nanometer-sized Pt_{50}-Sn_{50} Catalyst Particles Directly Deposited onto the Proton Exchange Membrane Surface

Chieh-Hao Wan[1,*], *Jyun-Ming Wei*[2], *Meng-Tsun Lin*[3], *Chien-Heng Lin*[3]

[1] Department of Electro-Optical and Energy Engineering, MingDao University, Changhua, Taiwan
[2] Department of Materials Science and Engineering, MingDao University, Changhua, Taiwan
[3] Institute of Materials Science and Engineering, National Chung Hsing University, Taichung, Taiwan
[*]E-mail: chiehhao@mdu.edu.tw

Received: 13 December 2010 / *Accepted:* 22 January 2011 / *Published:* 1 April 2011

A thin layer of nanometer-sized Pt_{50}-Sn_{50} catalyst particles deposited onto the proton exchange membrane (PEM) surface that served as methanol filter was prepared by the impregnation-reduction (IR) method to mitigate the methanol crossover and improve the utilization efficiency of methanol fuel. The mitigation of methanol crossover and performance of MEA containing this Pt_{50}-Sn_{50} layer had been measured and compared to those of normal-MEA which had no treatment on PEM. This paper investigated and presented possible mechanism of the suppression of methanol crossover of the proposed MEA structure. SEM, X-ray, EDS and EPMA analysis were used to characterize microstructures, phases, chemical composition and distributions of the obtained electrocatalyst layers. Methanol crossover rate in a DMFC was determined by measuring the CO_2 concentration at the cathode exhaust in real time. The result demonstrated that the MEA with a layer of nanometer-sized Pt_{50}-Sn_{50} catalyst particles suppressed methanol crossover by up to 17% more than that of the normal-MEA, and improved MEA performance by 8% at 80℃. However, at 60℃ the MEA performance dropped by 8% although the mitigation of methanol crossover was also observed. The Pt_{50}-Sn_{50} layer in PEM acted both as a methanol filter and an electrode. The dual-role contributed to the suppression of methanol crossover and improvement of performance. Indeed, the reduction of conductivity of PEM with the existence of a Pt_{50}-Sn_{50} layer in PEM surface has negatively impacted the output cell performance, especially at 60℃.

Keywords: Methanol crossover, Impregnation-reduction method, nanometer-sized Pt_{50}-Sn_{50} catalyst, conductivity of PEM, methanol filter.

1. INTRODUCTION

Direct methanol fuel cells (DMFC) are attractive for transportation and portable applications for several reasons, e.g., easy refueling and simple fuel storage, elimination of fuel reforming, simplified system design, etc. Methanol crossover is one of the most critical barriers to the commercialization of DMFC [1-3]. This is because un-reacted methanol diffuses from anode to cathode through the Nafion® membrane, causes a mixed potential and reduces the cell performance as well as the fuel utilization. Furthermore, the crossed-over methanol poisons the cathode Pt catalyst and reduces the output current density. Therefore, the methanol crossover should be reduced to increase the efficiency and stability of DMFC before this technology can becomes commercially viable. In this respect, several approaches have been studied and reported that can suppresses methanol crossover. These approaches include: 1) the development of a new membrane with low methanol permeability without sacrificing the proton conductivity [4-11], 2) ion-exchanging appropriate amount of Ce^{4+} into the proton exchange membrane (PEM) [12], 3) making a barrier of methanol crossover of Pd metal layer that deposited on the PEM surface to form a sandwich structure [13-14], 4) dispersion of nanometer-sized Pt particles into the PEM to react the crossed-over methanol [15], and 5) using the electrodeposition technique to deposit the Pt nanowires into a Nafion membrane surface [16].

Recently, our laboratory has proposed a new approach to mitigate methanol crossover [3]. A reactive methanol filter containing a layer of Pt-Ru catalyst deposited in the PEM anode side surface using the impregnation-reduction (IR) method, has shown significant suppresses of methanol crossover and performance improvement. The filtering effect of reactive methanol filter depends on the catalyst reaction rate over the Pt-Ru catalyst at the PEM surface. Based on this result, it is important to understand the suppression of methanol crossover and the performance improvement using a different binary Pt-based electrocatalyst, such as Pt-Sn. The selection of Pt-Sn as the catalyst for reactive methanol filter is because the electrocatalyst activity of Pt-Ru and Pt-Sn toward methanol is better than that of other binary Pt-based electrocatalyst such as Pt-Re, Pt-W et. al [18-19]. Furthermore, the Pt-Sn electrocatalyst is cheaper than Pt-Ru, lowering the DMFC's cost and make it more feasible for commercialization.

This paper presented a method that deposited an inner catalyst layer containing nanometer-sized Pt_{50}-Sn_{50} catalyst particles on the PEM anode side surface using the impregnation-reduction method (IR), to mitigate methanol crossover and improve the fuel utilization as well as the cell performance. Figure 1 shows the proposed PEM and MEA structures. The effects of a layer of Pt_{50}-Sn_{50} catalyst deposited on the PEM anode side on the suppression of methanol crossover and the MEA performance are discussed. The possible mechanism of the suppression of methanol crossover for the proposed MEA structure is also investigated.

2. EXPERIMENTAL DETAILS

Figure 1 presents the proposed MEA structure, which is denoted as MEA-Pt-Sn, containing the Pt_{50}-Ru_{50} anode, Pt_{50}-Sn_{50} inner catalyst layer on the Nafion membrane surface and Pt cathode.

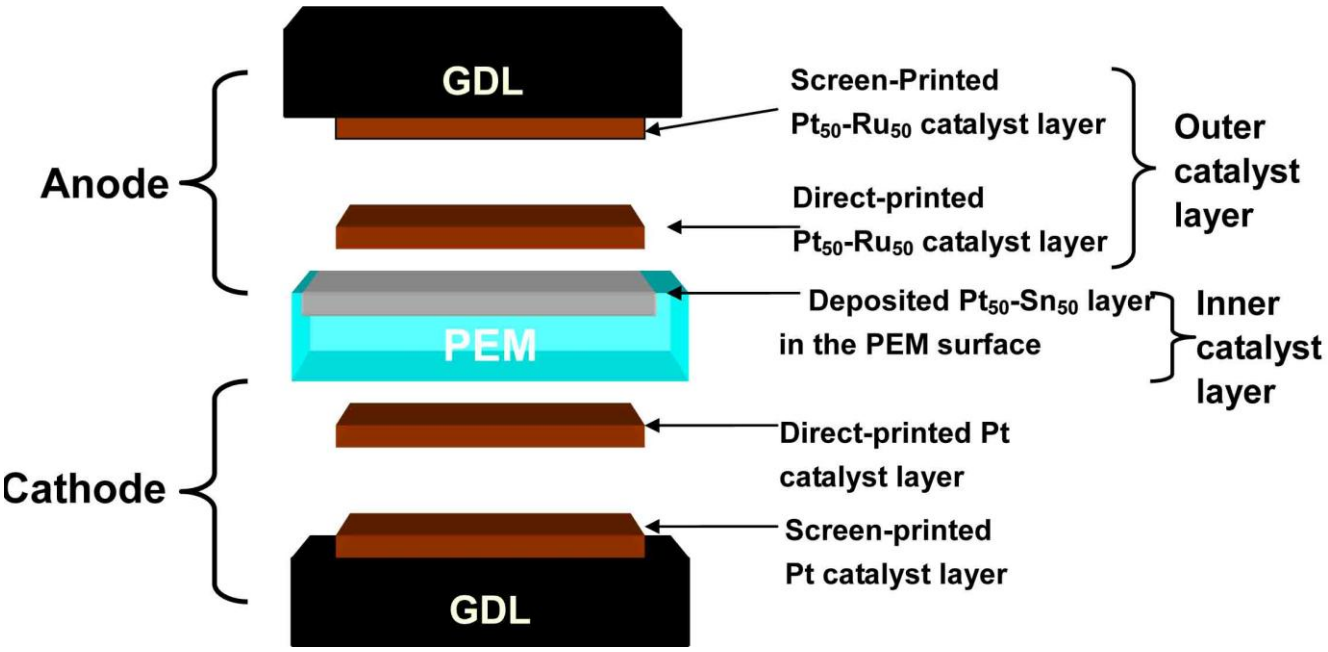

Figure 1. Diagram of the proposed anode and MEA structure.

A layer of Pt-Sn (0.90 mg Pt_{50}-Sn_{50} cm^{-2}) deposited onto the membrane surface is acted as a reactive methanol filter. The anode comprises a screen-printed Pt_{50}-Ru_{50} layer on the gas diffusion layer (GDL) and a direct-printed Pt_{50}-Ru_{50} layer on proton exchange membrane (PEM) with resulted anode loading of 3.00 mg Pt_{50}-Ru_{50} cm^{-2}. The cathode consists of a screen-printed Pt layer on the GDL and a direct-printed Pt layer on PEM with resulted cathode loading of 3.30 mg Pt cm^{-2}. In order to understand the effect of a Pt-Sn layer on the mitigation of methanol crossover and cell performance, we prepared a normal-MEA that contains PEM without any treatment and has the identical anode and cathode as that of MEA-Pt-Sn. Table 1 lists the loadings of anode and cathode for both MEAs.

Nafion 117 (DuPont, Inc., USA) was used as a polymer electrolyte membrane in each case. Before they were used, each membrane was first boiled in 3~5% hydrogen peroxide and then boiled in 0.5M sulfuric acid. It was then washed in reagent-grade water and finally stored in water.

2.1. Preparation of a Pt-Sn layer deposited on PEM surface

The reagent-grade water, produced using a Milli-Q SP ultrapure-water purification system from Nihon Millipore Ltd., Tokyo, was used as the solvent in all reactions. The pre-treated Nafion-117 was placed on the armed-side of a reactor designed in-house in order to provide anode-side only deposition. 0.1192g of $SnCl_2$ (Acros Organics) was added into 80ml of water and stirred for 20 minutes. The resulted solution was then moved to the reactor, followed by adding 14ml of HPLC-grade methanol in order to carry out the ion-exchange process of Sn precursor at 70℃ for 3 hours. Next, 0.0965g of $[Pt(NH_3)_4]Cl_2$ (Alrich®) was added into the $SnCl_2$ solution for 40 minutes. After no residue Pt and Sn ions were detected in the reactor, 0.3620g of $NaBH_4$ (Acros Organics) was added into methanol (3.8M) solution to conduct the reduction reaction at 70℃ for 30 minutes. After removing the $NaBH_4$

solution, the resulting Nafion membrane was treated with 1M H_2SO_4 at 80℃ for 2~3 hours to replace the non-reacted Pt and Sn precursors with protons to yield the fully H^+ form of PEM. Finally, the deposited Pt-Sn layer on PEM surface with loading of 0.90 mg cm^{-2}, as shown in table 1, was obtained when the H_2SO_4 had been fully washed out from PEM.

Table 1. Catalyst loadings of MEAs.

Sample code	Loading of Pt-Sn layer in PEM surface (mg Pt_{50}-Sn_{50} cm^{-2})	Anode loading (mg Pt_{50}-Ru_{50} cm^{-2})	Cathode loading (mg Pt cm^{-2})
MEA-Pt-Sn	0.90	3.00	3.30
Normal-MEA	**----**	**3.00**	**3.30**

2.2. Preparation of anode and cathode

The backing layer was prepared by screen-printing the carbon powder (Vulcan XC-72) solution containing 5% Nafion solution (DuPont) onto the carbon cloth. The anode catalyst ink consisted of aqueous dispersions of Pt_{50}-Ru_{50} (Alfa Aesar), 5% Nafion solution and isopropanol, while the cathode ink composed of aqueous dispersions of 20%Pt/C (BASF Fuel Cell), 5% Nafion solution and isopropanol. The detailed preparation procedures were described in [3, 17]. The total anode loading that produced from Pt_{50}-Ru_{50} catalyst layer on GDL and PEM surface was 3.00 mg Pt_{50}-Ru_{50} cm^{-2}, while the total cathode loading was 3.30 mg Pt cm^{-2}, as shown in table 1.

2.3. Preparation of MEA-Pt-Sn and normal-MEA

The Nafion membrane containing a Pt_{50}-Ru_{50} layer that was directly printed on the anode side and a Pt layer on the cathode side was placed between the two GDL electrodes. The MEA-Pt-Sn was finally produced by applying a pressure of 5~6 MPa at 139℃ for 1.7 minutes. The anode and cathode of normal-MEA was identical to that of MEA-Pt-Sn and prepared by the same procedure described in section 2-2. The PEM without Pt-Sn layer was placed between the two GDL electrodes. Hot-pressing this sandwich structure with a pressure of 5-6 MPa at 139℃ for 1.7 minutes formed the normal-MEA.

2.4. Characterization of Pt-Sn layer

The surface morphology, thickness and distributions of the Pt-Sn layers on Nafion membrane surface were characterized by a field emission scanning electron microscope, FESEM (JEOL, JSM-6700F), with an energy-dispersive spectrometer, EDS (OXFORD INSTRUMENTS, INCAx-sight 7557). The compositions of Pt-Sn layer were determined through an electron probe micro-analysis, EPMA (JEOL, JXA- 8500F). The PANalytical X-ray diffractometer X' Pert Pro using CuKα radiation

source operating at 40kV and 30mA was used to investigate the X-ray diffraction (XRD) patterns of the deposited Pt-Sn layers.

2.5. Evaluation of MEA

The performance evaluation of MEA was conducted through a single cell test fixture ($5cm^2$), supplied by Electrochem Inc., USA, with serpentine flow pattern on graphite plates. 2M methanol as anode fuel and dry oxygen gas as cathode fuel were fed into the test fixture at flow rates of 1 and 400 ml min^{-1}, respectively. The quantity of crossed-over methanol at the cathode side was monitored by measuring the steady-state concentration of CO_2 in the cathode exhaust (after trapping water in an ice trap) using a CO_2 sensor. We assumed that the detected CO_2 at the cathode side was exclusively produced from the crossed-over methanol. Therefore, the crossover rate of methanol could be calculated from the amount of produced CO_2. All CO_2 concentration remains steady after 15 minutes into the test. The output current and voltage as well as the CO_2 concentrations at the cathode side were measured when the CO_2 concentration remains steady after 1 hour. The polarization curves and the suppression of methanol crossover of the DMFC were investigated at 60 and 80℃.

3. RESULTS AND DISCUSSION

3.1. Physicochemical characterization of Pt-Sn layer

Figure 2 showed the SEM image of a Pt-Sn layer deposited onto the Nafion membrane surface using the IR method. Nano-spheres particles with average size of 50±10nm are well-dispersed on the surface.

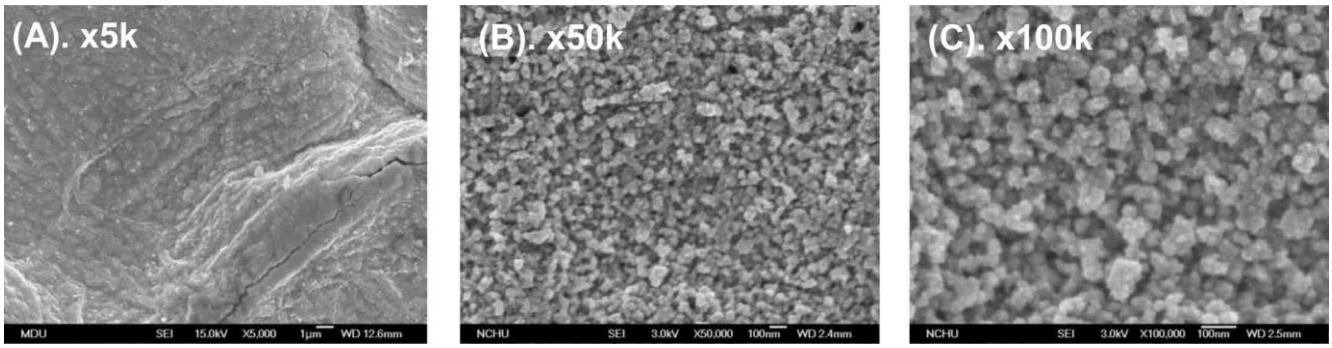

Figure 2. SEM pictures of Pt_{50}-Sn_{50} layer directly deposited onto the PEM surface using the IR method.

The X-ray diffraction (XRD) pattern at an X-ray incidence angle of 1° for this sample was shown in figure 3(b). In order to determine the alloy phase for Pt-Sn layer, we also measured the XRD patterns for pure Pt and Sn that deposited on the Nafion membrane surface at the same incidence

angle, as shown in figure 3(c) and 3(a). Figure 3(c) showed the characteristic peaks of Pt element at the positions of 40.07°, 46.34°, 67.69° and 81.55°, indicating the existence phase is pure Pt. Figure 3(a) demonstrated the characteristic peaks of Sn in the FCC structure, suggesting the existence of Sn with low degree of crystalline phase.

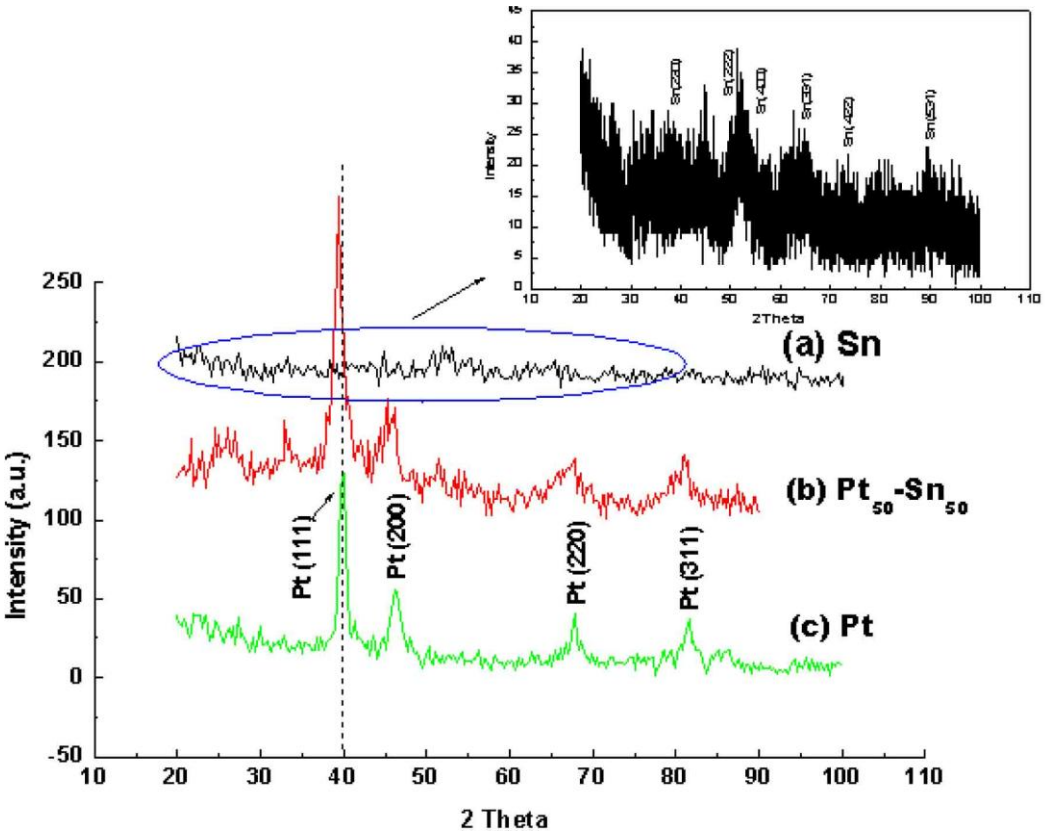

Figure 3. X-ray diffraction patterns of pure Pt, Sn and Pt-Sn alloy layers.

In Figure 3(c), the characteristic peak of Pt (111) face was strong and sharp at 40.07°. In contrast, no peak was observed at the corresponding peak position for pure Sn. Consequently, the Pt (111) face peak was chosen as the reference peak to confirm the existence of alloy phase by comparing the lattice constants of the obtained Pt-Sn and pure Pt samples. Calculation from Bragg's equation yielded a lattice constant of 3.920Å for pure Pt and 3.970Å for Pt-Sn, respectively. It is known that the lattice constant for pure Sn in FCC structure is larger than that of pure Pt [20]. The Sn atom was incorporated into the Pt FCC structure, then the lattice constant for Pt-Sn will become longer than that of Pt. Evidently, the lattice constant of Pt-Sn obtained from XRD was larger than that of pure Pt; confirming that the deposited layer was a Pt-Sn alloy phase.

The determination of the composition of the thin film was unable to obtain from the lattice parameter derived from XRD because of the substrate effect of the GID method. Electron probe micro-analysis (EPMA), on the other hand, can accurately measure the atomic ratio of the thin film, and was thus applied to determine the composition of it. The EPMA result (an average over 25 points)

demonstrated that the atomic ratio of Pt to Sn was about 50:50. The surface mapping of this layer using the EDS also showed similar results, suggesting well dispersion of Pt-Sn alloy phase in the layer.

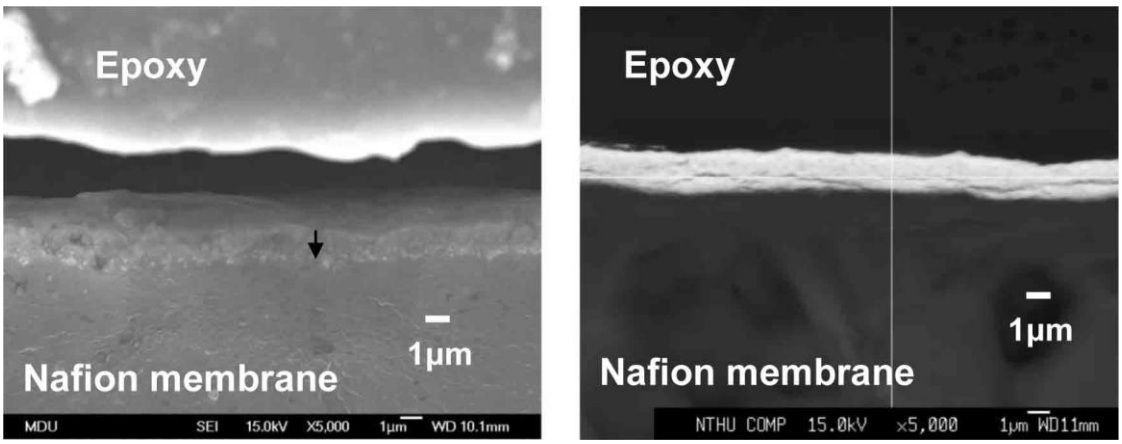

Figure 4. Cross-sectional SEM view (x5k) of Pt_{50}-Sn_{50} layer deposited onto the Nafion membrane surface in (A) the normal image mode; (B) the BEI image mode.

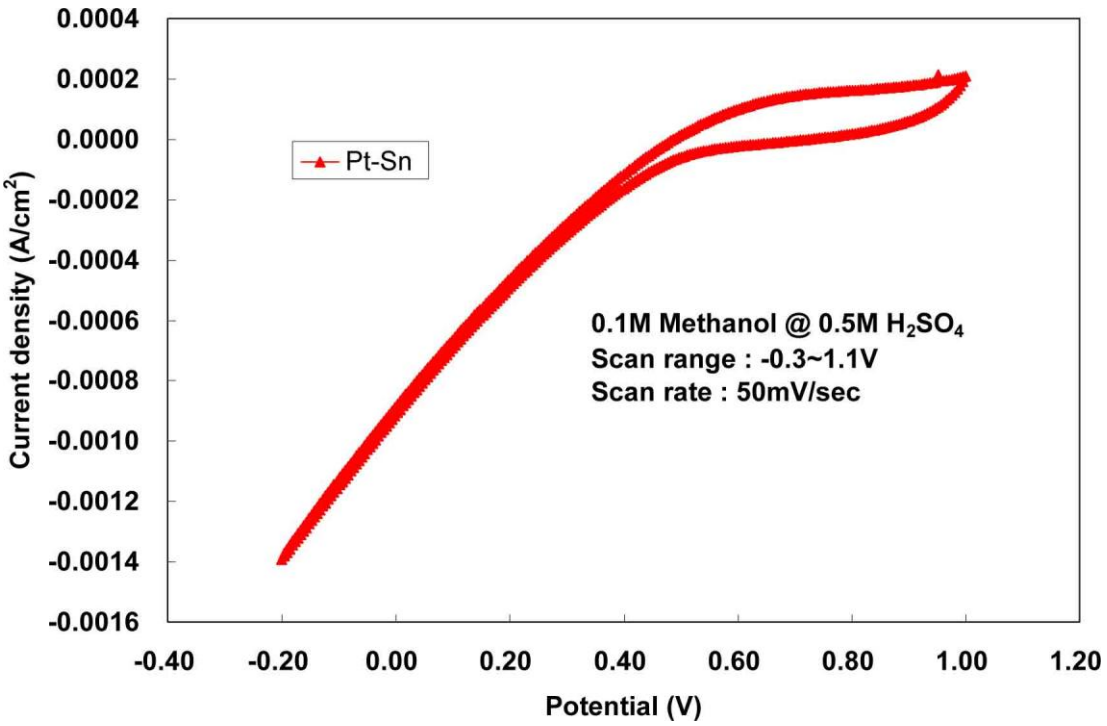

Figure 5. Cyclic voltammograms (CV) profiles for a Pt_{50}-Sn_{50} layer directly deposited onto the PEM surface tested in a solution of 0.5M H_2SO_4 and 0.1M methanol at 25℃.

The cross-sectional SEM view of the deposited Pt-Sn layer was shown in figure 4. Comparing the morphology on the surface, two different microstructures were found. Supporting results from the BEI image mode and EDS indicated that the upper layer was a metalized Pt-Sn layer with a thickness of 1.09μm. The Pt_{50}-Sn_{50} alloy layer concentrated at the surface of Nafion membrane that was adjacent

to the direct-printed Pt_{50}-Ru_{50} anode catalyst layer indicated a good contact between the deposited Pt-Sn layer and Pt_{50}-Ru_{50} anode catalyst layer. The density of Pt-Sn layer was calculated from dividing the Pt_{50}-Sn_{50} loading by the thickness of the deposited Pt-Sn layer, and yielded a layer density of 9.47g cm^{-3}.

Figure 5 presented the cyclic voltammograms (CV) profiles for a layer of Pt_{50}-Sn_{50} nano-particles directly deposited onto the Nafion membrane surface tested in a solution of 0.5M H_2SO_4 and 0.1M methanol at a scanning rate of 50 mV sec^{-1}. The onset potential of methanol oxidation occured at 0.37V and the current density at 0.65V was 0.083 mA cm^{-2} (0.092 A g^{-1}). This result indicated a layer of Pt_{50}-Sn_{50} directly deposited onto the PEM surface can oxidize methanol and function as an electrode. Note that the onset potential of methanol oxidation (0.37V) for Pt-Sn layer was higher than that of ethanol oxidation (0.31V) [17]. Furthermore, the peak current density for methanol oxidation was smaller than that of ethanol oxidation (0.11 mA cm^{-2}). This suggested the catalytic activity of Pt-Sn alloy toward the ethanol oxidation was better than that of methanol oxidation, which is consistent with literature [21].

3.2. Performance and suppression of methanol crossover

Figure 6 showed the CO_2 concentration detected at the cathode exhaust varied with the current density for MEA-Pt-Sn and normal-MEA. The solid and hallow symbols represented the MEA-Pt-Sn and normal-MEA operated at cell temperature of 80 and 60℃, respectively.

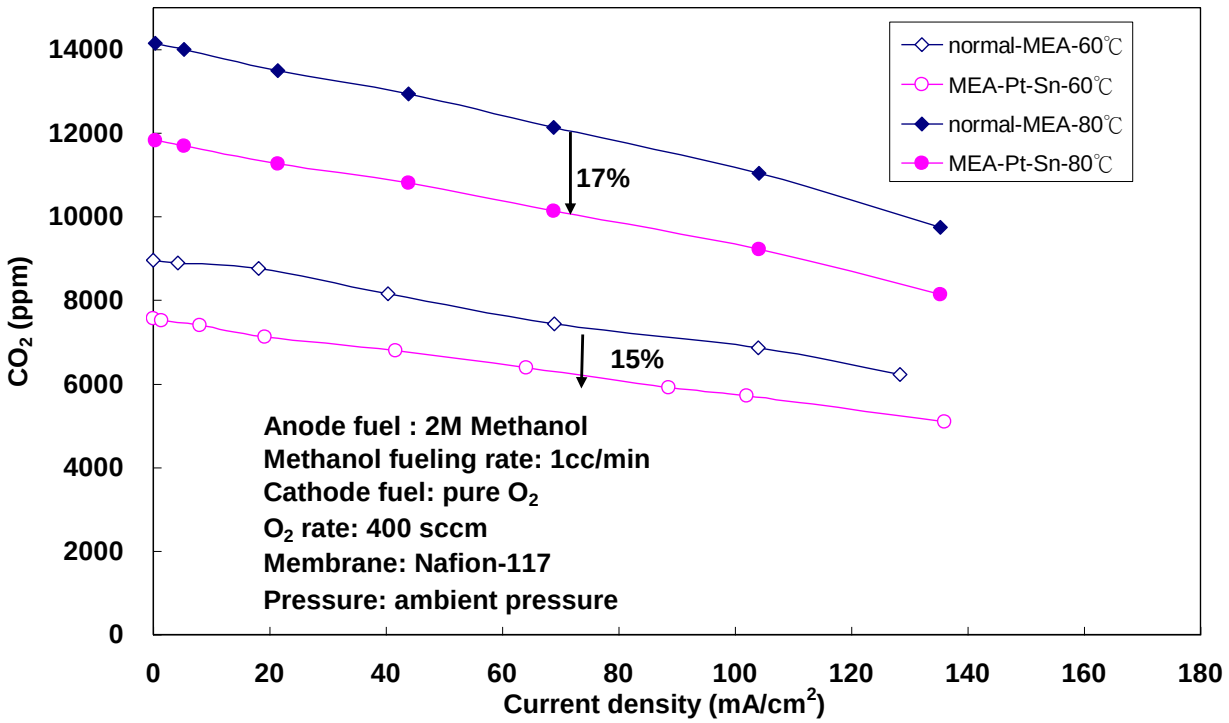

Figure 6. Steady-state CO_2 concentrations at the cathode exhaust varied with the current density for MEA-Pt-Sn and normal-MEA at 60℃ and 80℃, respectively.

The CO_2 concentrations for MEA-Pt-Sn at 80 and 60℃ were lower than that of normal-MEA by up to 17% and 15%, respectively, indicating the presence of a layer of Pt-Sn deposited onto the PEM surface suppressed the methanol crossover. Figure 7 showed the output voltage-current curves for MEA-Pt-Sn and normal-MEA at 80 and 60℃, respectively. The open-circuit voltages (OCVs) of MEA-Pt-Sn at 60℃ and 80℃ were 0.673V and 0.730V, while the OCVs of normal-MEA were 0.630V and 0.678V, respectively. It is known that the OCVs of DMFC increase with the occurrence of suppression of methanol crossover [22]. Therefore, the increments of OCVs of 0.043V and 0.052V at 60℃ and 80℃ for MEA-Pt-Sn were attributed to the mitigation of methanol crossover caused by a deposited Pt-Sn layer onto the PEM surface, which was consistent with the result in figure 6.

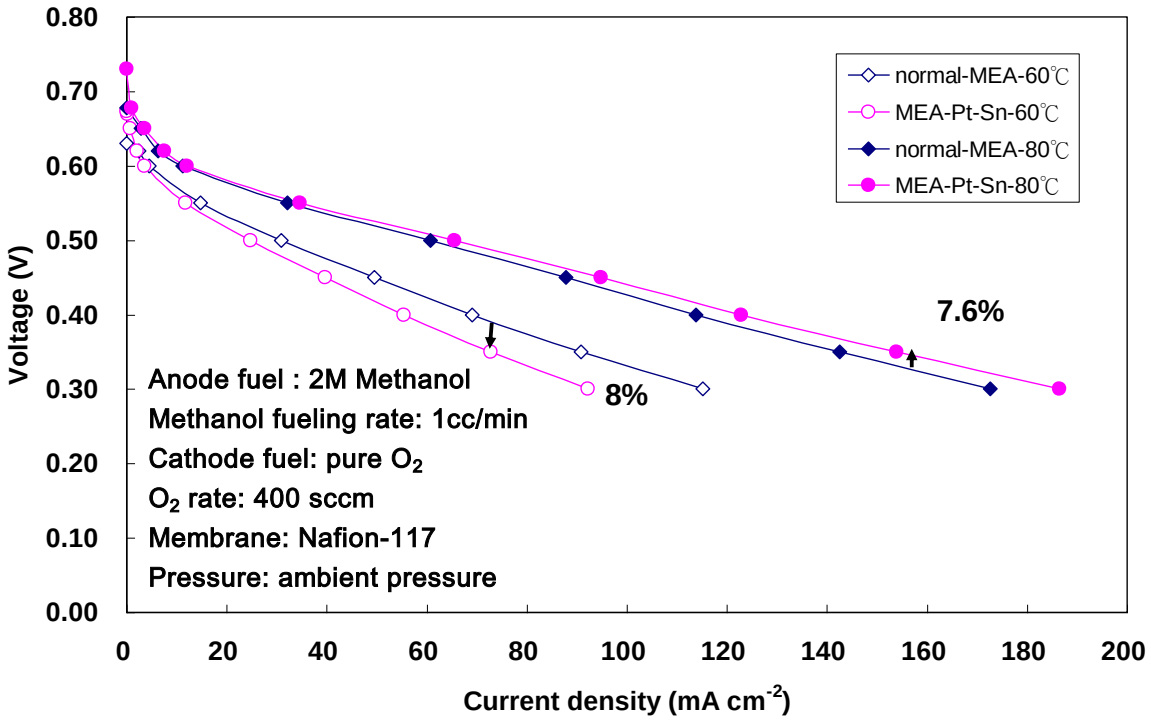

Figure 7. I-V curves of MEA-Pt-Sn and normal-MEA at 60℃ and 80℃, respectively.

Figure 7 indicated the performance of MEA-Pt-Sn at 80℃ was better than that of normal-MEA. However, it was lower than that of normal-MEA at 60℃. Comparing the potentials between the MEA-Pt-Sn and normal-MEA at 160 mA cm^{-2} under 80℃, the potential gain was up to 8% for MEA-Pt-Sn when compared to the normal-MEA. In contrast, the potential at 60℃ (@70 mA cm^{-2}) dropped about 8% as compared to the normal-MEA. A contrary performance results were obtained in different temperatures.

According to the results of CV and CO_2 concentration at the cathode side, a layer of Pt-Sn directly deposited onto the PEM surface was acted as an electrode and at the same time suppressed methanol crossover. The suppression mechanism of ethanol crossover reported in [17] can be applied to this study as well since the two MEAs have similar structure and composition as well as the Pt-Sn layer deposited on the PEM surface. The only difference was on the loadings of anode and cathode.

We postulated that a layer of Pt-Sn directly deposited onto the PEM surface reacted with the crossed-over methanol to produce the electrons, protons and CO_2. The produced electrons transferred to the cathode through the direct-printed Pt_{50}-Ru_{50} layer via external circuit, while the generated protons travelled to cathode through the PEM. In addition, this Pt-Sn layer functioned as an electrode at the interface between the PEM and anode Pt_{50}-Ru_{50} catalyst layer to oxidize the anode methanol fuel. Furthermore, the reduction of methanol crossover reduced the mixed potential effects [22]. The combination of these three effects improved the cell performance while mitigating the methanol crossover. Since the reduction of deleterious effect of crossover depended on the catalytic reaction between the crossed-over methanol and the Pt-Sn layer deposited on PEM, the improvement of cell performance and suppression of methanol crossover were strongly affected by the temperature, anode fuel concentration and the catalyst activity of a Pt-Sn layer deposited on PEM surface. Indeed, the ion-exchange in IR method that produced a Pt-Sn layer on PEM surface reduced the proton conductivity of PEM. The conductivity of PEM was dependent on the temperature, and the Nafion-117 membrane had the highest conductivity at 80℃, i.e. 0.042 S/cm. At 80℃, the catalytic reaction rate of a layer of Pt-Sn deposited on PEM surface and proton conductivity of this PEM were high, the performance improvement caused by the oxidation reaction of crossed-over methanol over the Pt-Sn layer and the reduction of mixed potential effects were higher than the resistance resulted from the existence of a Pt-Sn layer deposited on PEM surface. Therefore, the MEA-Pt-Sn with a layer of Pt-Sn deposited on PEM surface mitigated methanol crossover and improved the cell performance at 80℃. However, at 60℃, the reaction rate of a Pt-Sn layer and the proton conductivity of this PEM were relatively low. The performance improvement caused by the catalytic reaction of crossed-over methanol over the Pt-Sn layer and the reduction of mixed potential effect was lower than the increased resistance caused by producing a deposited Pt-Sn layer on PEM surface. Hence, the mitigation of methanol crossover with the reduction of cell performance at 60℃ was observed.

Comparing the results of this study and the results of similar MEA structure to MEA-Pt-Sn in [17], we discovered that the MEA with a layer of Pt-Sn deposited on PEM surface presented an improvement in performance at 60℃ in ethanol anode fuel, but suffered from reduction of performance in methanol fuel. In contrast, at 80℃, the performance improvement had been observed for both ethanol and methanol fuel. The result obtained was different for methanol and ethanol fuel at 60℃ because of three reasons.

First, the crossed-over ethanol had smaller effect on the cathode performance due to both ethanol's smaller permeability through Nafion® membrane and its slower electrochemical oxidation kinetic over Pt/C cathode [22]. This reduced the mixed potential effect and showed a lower depression of performance than that of the methanol fuel. Second, the Pt-Sn alloy was a better catalyst for ethanol as compared to methanol. Therefore the catalytic ability of a layer of Pt-Sn alloy towards ethanol was superior to methanol even at low temperature such as 60℃. Third, the Nafion® membrane porosity in ethanol was higher than that in methanol [22], and this caused a better ions transport characteristic in PEM for ethanol fuel which enhanced the cell performance accordingly. The combination of these three effects was the reason the MEA with a layer of Pt-Sn deposited on PEM can have an improvement of cell performance in ethanol fuel as compared to normal-MEA at 60℃, which was different from the methanol fuel.

4. CONCLUSION

A layer (with a thickness of 1.06μm) of nanometer-sized Pt_{50}-Sn_{50} alloy catalyst particles (average particle size is 50±10nm) deposited onto the Nafion® membrane anode side surface had been prepared by IR method under the proposed experimental conditions. This layer has good contact with the direct-printed Pt_{50}-Ru_{50} anode catalyst layer and serves as an inner catalyst layer that oxidizes the crossed-over methanol. The MEA with a layer of Pt_{50}-Sn_{50} alloy deposited onto the Nafion-117 membrane surface suppresses the methanol crossover up to 17% and improves the cell performance up to 8% as compared to the MEA without any treatment on PEM at 80℃. It is believed that a layer of nanometer-sized Pt_{50}-Sn_{50} alloy catalyst particles in PEM surface oxidizes the crossed-over methanol to produce electrons, protons and CO_2. The oxidation over the Pt-Sn layer reduces the amount of crossed-over methanol and thus reduces the mixed potential effect at cathode while improving the cell performance and utility efficiency of methanol fuel. Therefore, an inner catalyst layer in PEM with a deposited Pt-Sn layer functions as a reactive methanol filter. Its filtering effects are dependent on the temperature, anode fuel concentration and the catalyst activity of a Pt-Sn layer deposited on PEM surface. However, the existence of a layer of nanometer-sized Pt_{50}-Sn_{50} alloy catalyst particles in PEM surface does reduce the proton conductivity of PEM as ion-exchanging was applied to prepare the Pt-Sn layer. This effect reduces the cell performance. The effects of conductivity of PEM on the cell performance are evident at low temperature at 60℃ even though the mitigation of methanol crossover has also occurred.

A different performance result was obtained for the MEA with a layer of nanometer-sized Pt_{50}-Sn_{50} alloy deposited onto the Nafion membrane surface toward the methanol and ethanol anode fuel at 60℃. This MEA demonstrates a reduction of cell performance in methanol fuel while suppressing the methanol crossover because of the significant effect of crossed-over methanol on cathode performance, lower catalytic activity of Pt-Sn toward methanol and a lower Nafion® membrane porosity than ethanol. Therefore, the existence of a layer of Pt-Sn deposited on PEM surface shows a better performance in direct ethanol fuel cell at low temperature at 60℃.

ACKNOWLEDGEMENTS

The author would like to thank the National Science Council of Republic of China under the contract number of NSC 96-2221-E-451-008 -MY2 and NSC 99-2221-E-451-014-MY2 for financially supporting this research.

References

1. A.Heinzel, V. M. Barragan, *J. Power Sources*, 84 (1999) 70
2. G. T. Burstein, C. J. Barnett, A. R. Kucernak, K. R. Williams, *Catal. Today*, 38 (1997) 425
3. C. H. Wan, C. H. Lin, *J. Power Sources*, 186 (2009) 229
4. J. S. Wainright, D. Wang, R. F. Weng, M. Savinell, *J. Electrochem. Soc.*, 142 (1995) L121
5. M. Weng, J. S. Wainright, U. Landau, R. F. Savinell, *J. Electrochem. Soc.*, 143 (1996) 1260
6. J. T. Wang, S. Wasmus, R. F. Savinell, *J. Electrochem. Soc.*, 143 (1996) 1233
7. S. Wasmus, J. T. Wang, R. F. Savinell, *J. Electrochem. Soc.*, 142 (1995) 3825

8. P. Xing, G. P. Robertson, M. D. Guiver, S. D. Mikhailenko, S. Kaliaguine, *Polymer*, 46 (2005) 3257
9. F. Wang, M. Hickner, Y. S. Kim, T. A. Zawodzinski, J. McGrath, *J. Membr. Sci.*, 197 (2002) 231
10. H. Bai, W. S. Winston Ho., *J. Membr. Sci.*, 313 (2008) 75
11. M. A. Hickner, H. Ghassemi, Y. S. Kim, B. R. Einsla and J. E. McGrath, Chem. Rev. 104 (2004) 4587
12. V. Tricoly, *J. Electrochem. Soc.*, 145 (1998) 3798
13. C. Pu, W. Huang, K. L. Ley, E. S. Smoktin, *J. Electrochem. Soc.*, 142 (1995) L119
14. Z. Q. Ma, P. Cheng, T. S. Zhao, *J. Membr. Sci.*, 215 (2003) 327
15. H. Uchida, Y. Mizuno, M. Watanabe, *J. Electrochem. Soc.*, 149 (2002) A682
16. Z. X. Liang, T. S. Zhao, *J. Phys. Chem. C*, 111 (2007) 8128
17. C. H. Wan, C. L. Chen, *Int. J. Hydrogen Energy*, 34 (2009) 9515
18. D. H. Jung, C. H. Lee, C. S. Kim, *J. Power Sources*, 71 (1998) 169
19. A.K. Shukla, M. Neergat, P. Bera, V. Jayaram, M. S. Hegde, *J. Electroanal. Chem.* 504 (2001) 111
20. J. M. Leger, S. Rousseau, C. Coutanceau, F. Hahn, C. Lamy, *Electrochim. Acta*, 50 (2005) 5118
21. E. Antolini, *J. Power Sources*, 170 (2007) 1
22. S. Q. Song, W. J. Zhou, Z. X. Liang, R. Cai, G. Q. Sun, Q. Xin, V. Stergiopoulos, P. Tsiakaras, *Appl. Catal. B: Environ.*, 55 (2005) 65